HHS Public Access

Author manuscript

J Biol Chem. Author manuscript; available in PMC 2016 January 29.

Published in final edited form as:

J Biol Chem. 2002 November 1; 277(44): 41843–41849. doi:10.1074/jbc.M207111200.

Association of a Photoreceptor-specific Tetraspanin Protein, ROM-1, with Triton X-100-resistant Membrane Rafts from Rod Outer Segment Disk Membranes*

Kathleen Boesze-Battaglia[‡,§], **Janice Dispoto**[‡], and **Mary Anne Kahoe**[¶]

[‡]Department of Molecular Biology, School of Osteopathic Medicine, University of Medicine and Dentistry of New Jersey, Stratford, New Jersey 08084

[¶]Graduate School of Biomedical Sciences, University of Medicine and Dentistry of New Jersey, Stratford, New Jersey 08084

Abstract

This study reports the isolation and characterization of a Triton X-100-resistant membrane fraction from homogenates of rod outer segment (ROS) disk membranes purified free of the surrounding plasma membrane. A portion of the ROS disk membrane was found to be resistant to Triton X-100 extraction at 4 °C. This detergent-resistant fraction was isolated as a low buoyant density band on sucrose density gradients and exhibited an increase in light scattering detected at 600 nm. Biochemical analysis of the Triton X-100-resistant fraction showed it to be enriched in cholesterol and sphingomyelin relative to phospholipid and in phospholipid relative to protein compared with the soluble fraction. The Triton X-100-resistant membranes described herein did not arise simply from partial solubilization of the ROS disk membranes because detergent-treated low buoyant density fractions isolated from homogenates with octyl glucopyranoside had cholesterol and sphingomyelin content indistinguishable from that of solubilized ROS disk homogenates. Analysis of proteins associated with the Triton X-100-resistant fraction showed it to be enriched in the rim-specific protein ROM-1 and caveolin; surprisingly, the fusion protein peripherin/rds (where rds is retinal degeneration slow), also localized to the disk rim, was entirely absent from the membrane raft domain. The lipid profiles of the Triton X-100-resistant membranes were virtually identical in preparations homogenized in either the light or dark. Slightly more ROM-1 was recovered from samples prepared in the light (23%) than from samples prepared in the dark (13%), but peripherin/rds could not be detected in either preparation. When the Triton X-100-resistant membranes were treated with methyl-β-cyclodextran to deplete membrane cholesterol, the resultant membranes contained slightly lower levels of ROM-1, specifically in the dimeric form. Cholesterol depletion also resulted in the collapse of the large caveolin complex to monomeric caveolae. The results presented herein characterize a pool of ROM-1, a photoreceptor tetraspanin protein, that may play a regulatory role in peripherin/rds-dependent fusion.

*This work was supported by National Eye Institute Grant EY 10420 and an E. Matilda Ziegler Vision award. The costs of publication of this article were defrayed in part by the payment of page charges. This article must therefore be hereby marked "*advertisement*" in accordance with 18 U.S.C. Section 1734 solely to indicate this fact.

§ To whom correspondence should be addressed: Dept. of Biochemistry, University of Pennsylvania, School of Dental Medicine, 4001 Spruce St., Philadelphia, PA 19104-6003. Tel.: 215-898-9167; Fax: 215-898-3695; battagli@biochem.dental.upenn.edu..

Photoreceptor rod cells are responsible for vision under dim light. These unique post-mitotic cells are made up of a rod inner segment and a rod outer segment (ROS)[1] region. The ROS contains a stack of closed membranous sacs, referred to as disks, that contain the photoreceptor rhodopsin and that provide the requisite lipid environment for the initial events of phototransduction. There is a continual turnover of disk membranes and the proteins contained therein. Through coordinated processes of disk renewal at the base of the outer segment and disk shedding at the apical tip, the outer segment region is maintained at a constant length, and the physiologic function of light transduction is maintained (1). Interestingly, although the distribution of the major proteins within disks remains constant during the basal-to-apical transit of disks, a process that requires 10 days in the vertebrate rod cell, the lipid composition of the disks changes during this time. Specifically, the cholesterol content of the disks decreases by >50% as they age (2, 3), and the content of saturated fatty acid in the phospholipids increases (4). This same cholesterol heterogeneity is not observed in disk membranes isolated from an animal model of retinal degeneration, the Royal College of Surgeons rats (5). In addition to the loss of cholesterol from disks as they are apically transported, a tremendous sorting of lipid components occurs at the base of the ROS as new disks are formed from the surrounding ROS plasma membrane. The plasma membrane is found to be high in cholesterol (6) and squalene (7) and relatively enriched (compared with disks) in saturated fatty acids (4). Conversely, the mature disks are enriched in unsaturated fatty acids species, specifically docosahexanoic acid, 22:6 (6).

The sorting at the base of the ROS is not limited to lipid components, but includes the selective association of the cGMP channel, the GLUT-1 transporter, and the Na^{+}-Ca^{2+} exchanger (Refs. 8 and references therein) with the plasma membrane, while rhodopsin, guanylate cyclase, the ABCR protein, and two photoreceptor-specific tetraspanin proteins (peripherin/rds (where rds is retinal degeneration slow) and ROM-1) sort to the disk membrane (8). The unique protein complex consisting of peripherin/rds and its non-glycosylated homolog, ROM-1 (9–11), is localized exclusively to the bulbous ends of the disks, termed the rim region (12). Hydrodynamic evidence and mutagenesis studies have shown that peripherin/rds forms disulfide-linked dimers that assemble into homotetramers (13, 14). The tetramers associate into larger polymers of intermediate size, and polymerization appears to be inhibited by ROM-1 (13, 14). The peripherin/rds dimers complex noncovalently with ROM-1 homodimers to form heterotetrameric complexes, the precise function of which is unknown. Peripherin/rds participates in the maintenance of normal ROS disk membrane structure and in disk morphogenesis and shedding (Ref. 15 and references therein) and acts as a photoreceptor-specific fusion protein (16, 17).

Both peripherin/rds and ROM-1 belong to a growing family of proteins consisting of four transmembrane domains known collectively as tetraspanins (18). In various other cell types, tetraspanin proteins serve as molecular adapters in the assembly of protein complexes in membrane microdomains known as rafts (19, 20). The association between tetraspanin proteins and protein complexes falls into three categories, loosely associated such that, in a Triton X-100-soluble fraction, the complex is retained, or in a Triton X-100-soluble fraction,

[1]The abbreviations used are: ROS, rod outer segment(s); OG, octyl glucopyranoside; MOPS, 4-morpholinepropanesulfonic acid; mAb, monoclonal antibody; GARP, glutamic acid-rich protein.

the complex is not retained. Furthermore, the most tightly associated complexes are Triton X-100-resistant species that are isolated as membrane rafts (18). To understand the nature of the noncovalent association between peripherin/rds and ROM-1, we investigated the distribution of these two proteins in ROS disk membrane-specific membrane rafts.

The lateral organization of lipids within ROS membranes has been a subject of intense investigation over the past 2 decades (for reviews, see Refs. 21 and 22). More recently, the concept of lateral organization of lipids has been refined to include their role as functional domains within membranes with the recognition of separate liquid-ordered phases embedded in the liquid-disordered matrices in the bilayer (19). These more ordered liquid phases, known as rafts, are described as unique assemblies of cholesterol, sphingomyelin, and saturated lipids (23, 24). They can be readily isolated in most cells as Triton X-100-resistant species at low temperature. A correlation between lipid organization in the context of a membrane raft, phototransduction, and lipid and protein sorting is in the early stages of characterization. Recent model membrane studies suggest that cholesterol is necessary for the recruitment of polyunsaturated fatty acids by rhodopsin into membrane microdomains (25). Similar studies also demonstrated the requirement for specific lipids in the activation process of rhodopsin (26–28), in transducin binding (29), and in phosphodiesterase activation (30).

Rafts are involved in a variety of transport, signaling, and differentiation processes. Membrane rafts are characterized by a number of well defined criteria, the most essential of which are their high cholesterol-to-phospholipid content, high sphingomyelin content, low buoyant density, light scattering properties, and unique protein composition (19, 20, 31). Although other investigators have isolated what appear to be low buoyant density Triton X-100-resistant membrane fractions from ROS with unique protein compositions, their analyses did not include all of the criteria to distinguish these as rafts (32, 33). The results presented herein provide the first biochemical lipid analysis of ROS-specific membrane rafts and document the selective association of ROM-1 and caveolin with this raft species. To our surprise, membrane rafts isolated from purified ROS disk membranes appear to selectively contain ROM-1, and not peripherin/rds.

EXPERIMENTAL PROCEDURES

Materials

Methyl-β-cyclodextran and Triton X-100 were purchased from Sigma. Octyl glucopyranoside (OG) and anti-α-transducin antibody was purchased from Calbiochem. Frozen dark-adapted bovine retinas were purchased from J. Lawson, Inc. (Lincoln, NE). Cholesterol, phosphatidylcholine, phosphatidylethanolamine, phosphatidylserine, and sphingomyelin were purchased from Avanti Polar Lipids (Birmingham, AL). Monoclonal antibodies 2B6 (against peripherin/rds), 1D5 (against ROM-1), and 4D2 (against opsin) were generous gifts from Dr. Robert S. Molday (University of British Columbia, Vancouver, British Columbia, Canada). Anti-GARP-1 and anti-GARP-2 antibodies were generous gifts from Dr. U. B. Kaupp (Institut für Biologische Informationsverarbeitung, Julich, Germany). Anti-caveolin-1 antibody was purchased from BD Biosciences.

Isolation of ROS Disk Membranes

ROS disk membranes were isolated free from ROS plasma membrane vesicles using ricin-agarose and differential sucrose gradient centrifugation essentially as described in detail previously (6). Briefly, intact ROS membranes were isolated from the 1.11–1.13 g/ml sucrose interface and treated with neuraminidase and ricin-agarose. The ricin-agarose-bound ROS were lysed overnight in ice-cold water. Because we did not treat with trypsin, the peripherin/rds-GARP interaction should not have been disrupted by these conditions (34). The disks were separated from plasma membrane bound to ricin-agarose on sucrose density gradients. The ROS plasma membrane composes only 6–8% of the total membrane in the ROS (Ref. 6 and references therein). Under the isolation conditions as described (6) ~7% of the total membrane is ricin-associated plasma membrane, suggesting minimal (<1%) plasma membrane association with the disks. The isolated ROS disk membranes were pelleted at 17,500 rpm for 25 min and resuspended in MOPS buffer (10 mM MOPS, pH 7.2, 60 mM KCl, 30 mM NaCl, 5 mM $MgCl_2$, 1 mM dithiothreitol, 5 μM aprotinin, and 1 μM leupeptin) and used immediately.

Isolation of Triton X-100-resistant Membrane Rafts

Triton X-100-resistant membrane rafts were prepared from isolated disk membranes essentially as described by Seno *et al.* (32). Disk membranes were suspended in MOPS buffer to a final protein concentration of 8–10 mg/ml. Triton X-100 (2%, w/v) was added to this suspension to a final concentration of 1% (w/v), and the suspensions were homogenized with three passes of a glass pestle through a glass Tenboeck tissue grinder. Homogenates were prepared in the light or dark. The homogenate was mixed with 1.23 ml of 2.4 M sucrose to yield a final sucrose concentration of 0.9 M and transferred to an SW 41 centrifuge tube. The sample was overlaid with sucrose solutions in MOPS buffer at decreasing sucrose concentrations of 0.8, 0.7, 0.6, and 0.5 M and centrifuged at 46,000 rpm for 20 h at 4 °C. The fractions were collected and analyzed for cholesterol, phosphate, and protein. In control experiments, an equal volume of disk membranes with identical phosphate and protein content were treated with 2% OG as described previously (35).

In some experiments, the isolated ROS disk membranes were depleted of cholesterol by treatment with methyl-β-cyclodextran for 30 min at 37 °C (36). Following methyl-β-cyclodextran treatment, the disk membranes were recovered by centrifugation and resuspended in MOPS buffer prior to solubilization with Triton X-100. For one study, the isolated low buoyant density rafts were treated with methyl-β-cyclodextran as described above. After cyclodextran treatment, the rafts were centrifuged at 50,000 rpm for 30 min, and the pellet was resuspended for cholesterol, phosphate, and protein assays and Western blot analysis.

Immunoprecipitation and Western Blot Analysis

Immunoprecipitation studies were performed as described (37). The isolated fractions from the sucrose density gradients were recovered, and 10 μl of the primary antibody (bovine anti-peripherin/rds monoclonal antibody (mAb) 2B6 or anti-ROM-1 mAb 1D5) was added to each of the samples and incubated overnight with rotation at 4 °C. Following immunoprecipitation with 150 μl of protein A-Sepharose, the complexes were washed five

times with Nonidet P-40 buffer and resuspended in 2× SDS-PAGE sample buffer containing β-mercaptoethanol. After heating at 85 °C for 10 min, the samples were centrifuged at 14,000 rpm for 30 s, and the immunoprecipitated complexes were separated by SDS-PAGE and transferred to nitrocellulose for Western blot analysis (17) or silver-stained (38). The immunoreactive bands were visualized using the ECL detection system (Amersham Biosciences). The molecular masses of the immunoreactive species were calculated using R_F measurements of molecular mass markers.

Analysis of Lipid Composition

Cholesterol was determined as described (39). Phosphate was measured as described (40) and modified (41). Lipids were extracted from the low buoyant density fractions as described (42). Prior to extraction of lipids from the solubilized membrane fractions, they were dialyzed for 48 h against two changes of 10 mM HEPES and 0.5 M NaCl to decrease the detergent concentration. In both cases, 90 ± 1.2% of the total phospholipid was extracted, indicating that the presence of any residual Triton X-100 in the solubilized fractions did not interfere with the lipid extraction. The chloroform extracts were evaporated under N_2 and resuspended in $CHCl_3$/MeOH (2:1). The lipids were resolved by sequential one-dimensional TLC on Silica Gel H chromatograms developed in chloroform/methanol/acetic acid/water (25:15:4:2). The plates were developed in the same solvent system three times in sequence as described (43). The spots were identified by comparison with the migration of known standards (phosphatidylcholine, phosphatidylethanolamine, phosphatidylserine, sphingomyelin, and cholesterol) following specific staining using Dragendorff, ninhydrin, and sulfuric acid charring. The spots were scraped, and total phosphate was determined as described above.

RESULTS

Characterization of the Lipid Composition of a Triton X-100-resistant Membrane Species Isolated from ROS Disk Membranes

To identify and characterize ROS disk membrane-specific detergent-resistant membranes, purified disk membranes were homogenized with 1% Triton X-100 at 4 °C in either the dark (designated T_D) or light (designated T_L) and fractionated by sucrose density gradient centrifugation. Samples prepared in the dark (T_D) had two bands: a low density diffuse white-yellow band at a sucrose density of 20.1 ± 2.2% (designated $F1_D$) and a nearly transparent red-orange band at 26.5 ± 1.4%, similar to the Triton X-100-soluble band described by Seno *et al.* (32). The low buoyant density bands resolved in the sample prepared in the light (T_L) appeared to be more diffuse; and on occasion, two bands were detected. The low density band called $F1_L$ corresponded to an average percent sucrose of 18.6 ± 1.18%; a Triton X-100-soluble band was detected at 26 ± 2.2% sucrose.

To distinguish between Triton X-100-resistant membranes and simply partial solubilization of the ROS disk membranes, disk membranes were homogenized in the nonionic detergent OG (35) in either the dark or light (designated OG_D and OG_L, respectively). In the OG_D samples, a very low buoyant density diffuse white-yellow band was present at 19.7 ± 0.76% sucrose. OG_L samples showed a similar banding pattern with a fraction isolated at 16.5 ±

3.8%. With both the OG_D and OG_L samples, diffuse OG-soluble bands were detected at sucrose densities of 27.0 ± 0.76 and 24.5 ± 3.8%, respectively. When the disk membranes were treated with a higher concentration of OG, above the critical micelle concentration of the detergent, these low density bands were not observed, suggesting that the majority of the disk membrane proteins were solubilized completely.

The low density fractions isolated from the T_D and T_L samples (called $F1_D$ and $F1_L$, respectively) exhibited peak light scattering at 600 nm (data not shown), and these samples had higher absorbance at 600 nm than the OG_D and OG_L samples and the solubilized fractions. The increased light scattering was mirrored by a substantial increase in the phospholipid-to-protein content of $F1_D$ and $F1_L$. The absorbance at 600 nm was lower in the OG_D and OG_L samples because the membranes were partially solubilized, thereby scattering less light.

The results from the lipid analysis of the various fractions are shown in Table I. The low density Triton X-100-resistant fractions $F1_D$ and $F1_L$ contained from 16 to 19% of the total isolated phospholipid. The cholesterol/phospholipid (mole/mol) ratio in the $F1_D$ and $F1_L$ samples was more than twice that in the OG-treated samples and in the solubilized fractions. Similarly, the sphingomyelin content of the $F1_D$ and $F1_L$ samples was greater than that of the OG_D and OG_L fractions. Sphingomyelin represents <2% of the total phospholipid in ROS membranes (44) and was no higher in the OG_D and OG_L samples. In contrast, the $F1_D$ and $F1_L$ fractions had a 2-fold higher sphingomyelin/phospholipid ratio.

The biophysical characteristics of the $F1_D$ and $F1_L$ fractions from the Triton X-100-treated samples correspond to those described previously for detergent-insoluble membrane raft-like microdomains or detergent-resistant membranes (18, 45, 46). The designation of the $F1_D$ and $F1_L$ fractions as membrane raft-like microdomains was further substantiated by the observed high cholesterol/phospholipid ratios and the high sphingomyelin/phosphate ratio in these fractions. In contrast, the low density fractions isolated from the OG-treated disks showed cholesterol/phospholipid ratios analogous to that in the soluble fraction and a sphingomyelin/phospholipid ratio consistent with incomplete solubilization of disks. Recently, using two different techniques, Seno *et al.* (32) and Nair *et al.* (33) isolated what they determined to be ROS disk membrane-specific rafts; however, the protein contents of their rafts appear to differ. These investigators failed to provide lipid analysis showing higher cholesterol/phospholipid or sphingomyelin/phospholipid ratios in their low density fractions indicating a raft-like species, thus making it difficult to directly compare the protein components of the ROS membrane rafts. Our results are the first to identify and characterize both the lipid profile and the tetraspanin protein profile of disk membrane rafts.

Analysis of ROS Membrane Proteins in Membrane Raft-like Microdomains

Immunoblot analysis showed that the $F1_D$ and $F1_L$ fractions had a unique protein composition compared with the soluble fractions, especially in contrast to the OG_D and OG_L samples, as shown in Fig. 1 (*A*–*D*). Both the $F1_D$ and $F1_L$ fractions were found to contain a protein with a molecular mass of 37 kDa that was immunoreactive with anti-ROM-1 mAb 1D5 (Fig. 1*A*). ROM-1 was also detected in the soluble fractions, as expected. Based on a comparison of the intensities of the two immunoreactive bands, slightly higher levels of

ROM-1 were detected in the samples treated in the light (23% of total ROM-1) than in those treated in the dark (13% of ROM-1). A corresponding decrease in the intensity of the amount of ROM-1 in the soluble dark fraction was observed. 63- and 37-kDa proteins were also observed to be immunoreactive with anti-ROM-1 mAb 1D5 in the OG-treated samples (OG_D and OG_L). These immunoreactive bands most likely correspond to a ROM-1 monomer (37 kDa) and a ROM-1 homodimer and/or a peripherin/rds heterodimer (63 kDa). The OG-treated low buoyant density fractions contained 33 and 43% of the total ROM-1 when the samples were prepared in the dark and light, respectively. These percentages are consistent with the phospholipid content of the OG-treated samples, suggesting partial solubilization of these membranes, not detergent resistance.

Because ROS peripherin/rds has been shown to form a heterotetrameric complex with ROM-1, it was initially expected that the $F1_D$ and $F1_L$ fractions would also contain peripherin/rds. Most surprising was the observation that no immunoreactivity was detected with anti-peripherin/rds mAb 2B6 in these fractions (Fig. 1*B*). In addition, no peripherin/rds immunoreactivity was observed with polyclonal antibody to peripherin/rds (data not shown). Peripherin/rds was, however, detected in the Triton X-100-soluble fraction and in the OG-treated low density and soluble fractions. (Fig. 1*B*). The Triton X-100-resistant fractions $F1_D$ and $F1_L$ (data not shown) were found to contain rhodopsin, as shown in Fig. 1*C*. In our preparations in the light, we observed large amounts of aggregated rhodopsin in the low buoyant density bands, leading us to question how much of that rhodopsin was truly raft-associated.

The isolated ROS membrane raft-like microdomains were also assayed for the presence of caveolin. As shown in Fig. 1*D*, both the high molecular mass 314-kDa caveolae and the low molecular mass 22-kDa caveolin monomers were detected in the Triton X-100-treated $F1_D$ and $F1_L$ samples. Very little caveolin was detected in the $F1_L$ sample. In contrast, both caveolae and the lower molecular mass (22 kDa) caveolin monomer were detected in the Triton X-100-soluble fractions. In the presence of OG, the predominant form was the low molecular mass (22 kDa) form of caveolin, as expected based on previous studies (47, 48).

To further substantiate the absence of detectable levels of peripherin/rds in the ROM-1-enriched membrane raft-like species ($F1_D$ and $F1_L$), the samples were immunoprecipitated with either anti-ROM-1 mAb 1D5 or anti-peripherin/rds mAb 2B6 (Fig. 2, *A* and *B*). When the samples were immunoprecipitated with anti-peripherin/rds mAb 2B6 and probed with anti-ROM-1 mAb 1D5, no detectable immunoreactivity was observed in the $F1_D$ (Fig. 2*A*) and $F1_L$ (data not shown) fractions. However, a 36-kDa immunoreactive band corresponding to ROM-1 was observed in disk membranes (10). In contrast, when the samples were immunoprecipitated and probed with anti-ROM-1 mAb 1D5, a 37-kDa band was observed in both the $F1_D$ (Fig. 2*B*) and $F1_L$ (data not shown) fractions as well as in the soluble fractions. No detectable immunoreactivity was observed when the anti-ROM-1 mAb 1D5 immunoprecipitate from the $F1_L$ and $F1_D$ samples was probed with anti-peripherin/rds mAb 2B6. As expected, disk membranes were found to be immunoreactive with both anti-ROM-1 mAb 1D5 and anti-peripherin/rds 2B6, as shown previously (10).

Sphingomyelin/cholesterol-enriched membrane raft-like microdomains may be depleted of cholesterol with methyl-β-cyclodextran as described (32, 36). When the $F1_D$ and $F1_L$ fractions were treated with methyl-β-cyclodextran, the cholesterol/phospholipid ratio in the membrane rafts decreased from 0.24 ± 0.09 to 0.10 ± 0.03. As shown in Fig. 3, lower levels of ROM-1 in the dimeric form were detected in the cholesterol-depleted samples compared with controls. When the cholesterol-depleted $F1_D$ samples were analyzed for caveolin, only the lower molecular mass caveolin species was present. This result is not unexpected because the formation of high molecular mass caveolin requires a cholesterol-enriched membrane environment (48). Again, no detectable levels of peripherin/rds were observed. α-Transducin was found in both untreated and methyl-β-cyclodextran-treated samples (data not shown), as described previously (32). Collectively, the results presented herein have provided a reference point based on lipid analysis for subsequent characterization of ROS membrane rafts. In addition, we have provided clear evidence showing that ROS ROM-1 is a raft-specific protein, a portion of which does not form noncovalently linked tetramers with peripherin/rds.

DISCUSSION

In this work, we have provided the first lipid analysis supporting the isolation of a Triton X-100-resistant membrane fraction as a membrane raft in retinal ROS disk membranes. This Triton X-100-resistant membrane fraction composes 15–20% of the total membrane phospholipid and has high light scattering at 600 nm and a high characteristic cholesterol/phospholipid ratio and a corresponding high sphingomyelin content and therefore meets the biochemical criteria for designation as a membrane raft. Most intriguing is the observation that the ROS disk membrane rafts contain ROM-1, but do not contain the other disk rim protein, peripherin/rds. This result was unexpected because ROM-1 and peripherin/rds form heterotetramers *in vivo* (10) such that the amount of ROM-1 available to form this complex may be limiting. Early studies of transiently transfected COS cells showed that the interaction between peripherin/rds and ROM-1 requires coexpression. When COS cells were transfected individually with peripherin/rds or ROM-1, and cell extracts containing the singly expressed protein were combined, no measurable association was observed between peripherin/rds and ROM-1 (10). Similar results have been observed in our laboratory using polarized Madin-Darby canine kidney cells (data not shown). In light of the current findings, these early results may be due to the presence of ROM-1 in COS cell membrane rafts. Our studies also found no detectable levels of GARP-1 or GARP-2 associated with the disk membrane-specific rafts (data not shown), a result not entirely unexpected because no peripherin/rds was detected in these samples.

Collectively, these results lend further support to the hypothesis that peripherin/rds exists in ROS in distinct “pools” potentially with differing functions: as a large oligomeric complex necessary for the formation of a disk rim (Ref. 15 and references therein), as a protein tethering disk membranes to the plasma membrane through GARP (34), and as a membrane fusion protein (16, 17). Similar multifunctional properties have been reported for a group of tetraspanin proteins known as connexins (31). The role ROM-1 plays through its association with peripherin/rds in a tetrameric complex remains to be determined, although we have provided evidence suggesting that ROM-1 plays an accessory role in peripherin/rds-

dependent fusion (49). These studies are the first to show that ROS disk membrane rafts contain caveolae, in addition to ROM-1, and that the high molecular mass caveolin complex is reduced to monomeric caveolae upon membrane cholesterol depletion (Fig. 4).

Investigators have suggested that some Triton X-100-resistant membrane species are due to partial solubilization of the membranes (35) or protein oligomerization (50). To exclude this possibility, OG was used in place of Triton X-100. When the purified disk membranes were treated with 1% OG (a concentration below the critical micelle concentration), a low buoyant density membrane species was isolated at a position similar to that of the Triton X-100-resistant membrane rafts. However, this membrane species had a cholesterol/phospholipid ratio and a sphingomyelin content similar to those of the soluble fraction, with no preferential association of protein with the OG-treated fraction. This partially solubilized membrane could be completely solubilized when the concentration of OG was increased above the critical micelle concentration. Similar partially solubilized species were also isolated from cells upon treatment with OG in contrast to the isolation of Triton X-100-resistant membranes (35). Collectively, the comparison between fractions isolated using the two different detergents further confirms that the Triton X-100-resistant species are most likely membrane rafts.

The cholesterol content of the disk membrane-specific rafts is consistent with that seen in other cell types. Although the cholesterol/phospholipid ratio in the disk rafts (0.24) (Table I) is lower than in platelets (1.2) (51). In both cases, the membrane rafts have two times more cholesterol than the native cell membranes. In addition, the percent of total cholesterol in disk rafts is 10–12% of the total, identical to 10% of the total detected in erythrocytes (52) and intestinal epithelial cells (53). Thus, although ROS membranes have a lower cholesterol/phospholipid ratio than other cells types, the relative distribution of cholesterol in disk membrane rafts in comparison with the non-raft membranes is similar to that observed in other systems.

Early freeze-fracture studies of mouse, frog, and bovine photoreceptors using the fillipin binding technique indicated the presence of cholesterol-enriched fillipin-induced pits confined to particle-free patches within the plasma membrane and in newly formed disk membranes (54). These pits were attributed to a temperature-induced lateral phase separation in these membranes. In light of our present study, this definition may be expanded, and the freeze-fracture observations appear consistent with the formation of cholesterol-enriched membrane microdomains similar to those described herein. Assuming that Andrews and Cohen (54) were looking at membrane raft domains in photoreceptor cells, we can predict that the raft-like species isolated here biochemically are most likely analogous to those observed microscopically. That being the case, these fillipin-induced pits or rafts were localized to the plasma membrane surface and were seen most often in the newly forming disks of mice and were only observed in frogs in these same locations when the frogs were reared at 37 °C. Because the ability of fillipin to partition uniformly throughout the entire length of the ROS maybe questionable, the rafts are most likely not limited *in vivo* to those areas detected by these freeze-fracture studies. The work of Andrews and Cohen (54) was used as the basis for separating ROS disk membranes based on age and spatial distribution using digitonin (2, 3). In light of the current findings, those experiments

should be expanded to include the isolation and characterization of membrane rafts in the disks as a function of age. The removal of endogenous cholesterol as disks age is unique to the ROS disk membranes. Because cholesterol is lost as disks are displaced up the length of the ROS, this lipid provides an ideal *in vivo* regulatory system for the control of cellular processes requiring membrane rafts.

When the rafts were depleted of cholesterol using methyl-β-cyclodextran, a slight decrease was observed in the ROM-1 levels, specifically in the amount of dimer. The phospholipid/protein ratio of the cholesterol-depleted species was unchanged, although the total phosphate content was less, suggesting a reduced recovery of membrane. However, the levels of α-transducin were unchanged following cholesterol depletion. Based on the present results, selective removal of a portion of ROM-1 upon cholesterol depletion cannot be ruled out. Further studies using sedimentation velocity analysis are required to characterize the oligomeric forms of both ROM-1 in the raft species and peripherin/rds in the non-raft membranes. It is tempting to speculate that the methyl-β-cyclodextran-induced removal of cholesterol mimics the loss of cholesterol from disk membranes that occurs naturally as disks age and are displaced apically along the ROS (2, 3). Because caveolin-1 also binds both sphingomyelin and cholesterol *in vitro* and *in vivo*, its localization to the ROS disk membrane is important to the elucidation of cholesterol trafficking within the ROS. In addition, Ghalayani *et al.* (55), have described the association of members of the Src family of kinases with ROS membranes. Such Src kinases are components of the caveola signaling machinery and are proposed to play a role in transduction processes within the disk membranes. In follow-up studies, care must be taken to distinguish caveolae from membrane rafts using non-detergent-based techniques (56).

It has not escaped our attention that the data presented herein may lead to a reevaluation of the accepted stoichiometry between ROM-1 and peripherin/rds, which holds that there is a 2-fold excess of peripherin/rds over ROM-1. This stoichiometry is based upon analyses of the protein content of Triton X-100-soluble homogenates of ROS membranes (10, 11). Although the analyses were rigid, that portion of ROM-1 which is Triton X-100-resistant may have been inadvertently omitted from the sedimentation velocity analyses. It remains to be determined whether membrane raft-associated ROM-1 alters the accepted stoichiometry.

Within the context of retinal degenerative disease, no known mutations of ROM-1 have resulted in a disease phenotype; however, digenic mutations in peripherin/rds and ROM-1 have resulted in retinitis pigmentosa. The phenotype of the peripherin/rds-ROM-1 digenic forms of retinitis pigmentosa may depend on the association of ROM-1 with a membrane raft, thereby compromising the ability of ROM-1 to form viable interactions with peripherin/rds, a hypothesis presently not inconsistent with available sedimentation velocity analysis (14). In ROM-1 knockout mice (57), although normal outer segment formation is observed, the unusually large elongated shape of the ROS in these animals suggests a role for ROM-1 in mediating cell viability. Recent studies in our laboratory suggest that this phenotype may be due to the role of ROM-1 as an accessory in peripherin/rds-mediated fusion events (49). Collectively, the results presented suggest a slightly revised view of the disk rim, as shown schematically in Fig. 4.

REFERENCES

1. Young RW. Investig. Ophthalmol. Vis. Sci. 1976; 15:700–715. [PubMed: 986765]
2. Boesze-Battaglia K, Hennesey T, Albert AD. J. Biol. Chem. 1989; 264:8151–8155. [PubMed: 2722776]
3. Boesze-Battaglia K, Fliesler SJ, Albert AD. J. Biol. Chem. 1990; 265:18867–18870. [PubMed: 2229047]
4. Boesze-Battaglia K, Albert AD. Exp. Eye Res. 1989; 49:699–701. [PubMed: 2806432]
5. Boesze-Battaglia K, Organisciak D, Albert AD. Exp. Eye Res. 1994; 58:293–300. [PubMed: 8174652]
6. Boesze-Battaglia K, Albert AD. Exp. Eye Res. 1992; 54:821–823. [PubMed: 1623969]
7. Flielser SJ, Boesze-Battaglia K, Paw Z, Keller RK, Albert AD. Exp. Eye Res. 1997; 64:279–282. [PubMed: 9176062]
8. Molday RS. Investig. Ophthalmol. Vis. Sci. 1998; 39:2491–2513. [PubMed: 9856758]
9. Bascom RA, Manara S, Collins L, Molday RS, Kalnins VI, McInnes RR. Neuron. 1992; 8:1171–1184. [PubMed: 1610568]
10. Goldberg AFX, Moritz OL, Molday RS. Biochemistry. 1995; 34:14213–14219. [PubMed: 7578020]
11. Goldberg AFX, Molday RS. Biochemistry. 1996; 35:6144–6149. [PubMed: 8634257]
12. Arikawa K, Molday LL, Molday RS, Williams DS. J. Cell Biol. 1992; 116:659–667. [PubMed: 1730772]
13. Goldberg AFX, Loewen CJ, Molday RS. Biochemistry. 1998; 37:680–685. [PubMed: 9425091]
14. Loewen CJ, Molday RS. J. Biol. Chem. 2000; 275:5370–5378. [PubMed: 10681511]
15. Boesze-Battaglia K, Goldberg AFX. Int. Rev. Cytol. 2002; 216:183–226. [PubMed: 12019563]
16. Boesze-Battaglia K, Kong F, Lamba OP, Stefano FP, Williams DS. Biochemistry. 1997; 22:6835–6846. [PubMed: 9184167]
17. Boesze-Battaglia K, Lamba OP, Napoli A, Sinha S, Guo Y. Biochemistry. 1998; 37:9477–9487. [PubMed: 9649331]
18. Claas C, Stipp C, Hemler ME. J. Biol. Chem. 2001; 276:7974–7984. [PubMed: 11113129]
19. Simons K, Ikonen E. Nature. 1997; 387:569–572. [PubMed: 9177342]
20. Brown DA, Rose JK. Cell. 1992; 68:533–544. [PubMed: 1531449]
21. Razani B, Lisanti MP. Exp. Cell Res. 2001; 271:36–44. [PubMed: 11697880]
22. Brown DA, London E. Annu. Rev. Cell Dev. Biol. 1998; 14:111–136. [PubMed: 9891780]
23. Sargiacomo M, Sudol M, Tang Z, Lisanti MP. J. Cell Biol. 1993; 122:789–807. [PubMed: 8349730]
24. Brown DA, London E. J. Biol. Chem. 2000; 275:17221–17224. [PubMed: 10770957]
25. Polozova A, Litman BJ. Biophys. J. 2000; 79:2632–2643. [PubMed: 11053136]
26. Litman BJ, Niu SL, Polozova A, Mitchell DC. J. Mol. Neurosci. 2001; 16:237–242. [PubMed: 11478379]
27. Mitchell DC, Niu SL, Litman BJ. J. Biol. Chem. 2001; 276:42801–42806. [PubMed: 11544258]
28. Niu SL, Mitchell DC, Litman BJ. J. Biol. Chem. 2001; 276:42807–42811. [PubMed: 11544259]
29. Albert AD, Young JE, Paw Z. Biochim. Biophys. Acta. 1998; 1368:52–60. [PubMed: 9459584]
30. Boesze-Battaglia K, Albert AD. J. Biol. Chem. 1990; 265:20727–20730. [PubMed: 2174424]
31. Simons K, Toomre D. Nat. Rev. 2000; 1:31–39.
32. Seno K, Kishimoto M, Abe M, Higuchi Y, Mieda M, Owada Y, Yoshima W, Liu H, Hayashi F. J. Biol. Chem. 2001; 276:20813–20816. [PubMed: 11319214]
33. Nair KS, Balasubramanian N, Slepak VZ. Curr. Biol. 2002; 12:421–425. [PubMed: 11882295]
34. Poetsch A, Molday L, Molday RS. J. Biol. Chem. 2001; 276:48009–48016. [PubMed: 11641407]
35. Nusrat A, Parkos CA, Verkade P, Foley CS, Liang TW, Innis-Whitehouse W, Eastburn KK. J. Cell Sci. 2000; 113:2363–2374. [PubMed: 10852816]

36. Christian AE, Haynes MP, Philips MC, Rothblat GH. J. Lipid Res. 1997; 38:2264–2272. [PubMed: 9392424]
37. Springer, HA. Current Protocols in Immunology. Coligan, JE.; Kruisbeck, AM.; Margulis, DH.; Shevach, EM.; Strober, W., editors. John Wiley & Sons, Inc.; New York: 1996. p. 8.3.1.-8.3.11.
38. Merrill CR, Goldman D, Van Keuran ML. Electrophoresis. 1982; 3:17–23.
39. Allain CC, Poon LS, Chan CSG, Richmond W, Fu PC. Clin. Chem. 1974; 20:470–475. [PubMed: 4818200]
40. Bartlett GR. J. Biol. Chem. 1959; 234:466–472. [PubMed: 13641241]
41. Litman BJ. Biochemistry. 1973; 13:2545–2554. [PubMed: 4350955]
42. Folch J, Lees M, Sloane Stanley GA. J. Biol. Chem. 1957; 226:497–509. [PubMed: 13428781]
43. Skipski VP, Peterson RF, Barclay M. Biochem. J. 1964; 90:374–380. [PubMed: 4284220]
44. Fliesler SJ, Anderson RE. Prog. Lipid Res. 1983; 22:79–131. [PubMed: 6348799]
45. Rietveld A, Simons K. Biochim. Biophys. Acta. 1998; 1376:467–479. [PubMed: 9805010]
46. Dorahy DJ, Lincz LF, Meldrum CJ, Burns GF. Biochem. J. 1996; 319:67–72. [PubMed: 8870650]
47. Anderson RG. Annu. Rev. Biochem. 1998; 67:199–225. [PubMed: 9759488]
48. Schubert A-L, Schubert W, Spray DC, Lisanti MP. Biochemistry. 2002; 41:5754–5764. [PubMed: 11980479]
49. Boesze-Battaglia K, Stefano FP, Sinha S, Lamba OP. Investig. Ophthalmol. Vis. Sci. 1999; 40:4909.
50. Wong V. Am. J. Physiol. 1997; 273:C1859–C1863. [PubMed: 9435490]
51. Bodin S, Giuriato S, Ragab J, Humbel BM, Viala C, Vieu C, Chap H, Payraste B. Biochemistry. 2001; 40:15290–15295. [PubMed: 11735411]
52. Samuel BU, Mohandas N, Harrison T, McManus H, Rosse W, Reid M, Haldar K. J. Biol. Chem. 2001; 276:29319–29329. [PubMed: 11352913]
53. Martin-Belmonte F, Arvan P, Alonso M. J. Biol. Chem. 2001; 276:49337–49342. [PubMed: 11673461]
54. Andrews LD, Cohen AI. J. Cell Biol. 1983; 97:749–755. [PubMed: 6411740]
55. Ghalayani AJ, Desai N, Smith K, Holbrook RM, Elliott M, Kawakatsu H. J. Biol. Chem. 2002; 277:1469–1476. [PubMed: 11705988]
56. Fra A,M, Williamson E, Simons K, Parton RG. J. Biol. Chem. 1994; 269:30745–30748. [PubMed: 7982998]
57. Clarke G, Goldberg AFX, Vidgen D, Collins L, Ploder L, Schwarz L, Molday L, Rossant J, Szel A, Molday RS, Birch DG, McInnes RR. Nat. Genet. 2000; 25:67–73. [PubMed: 10802659]

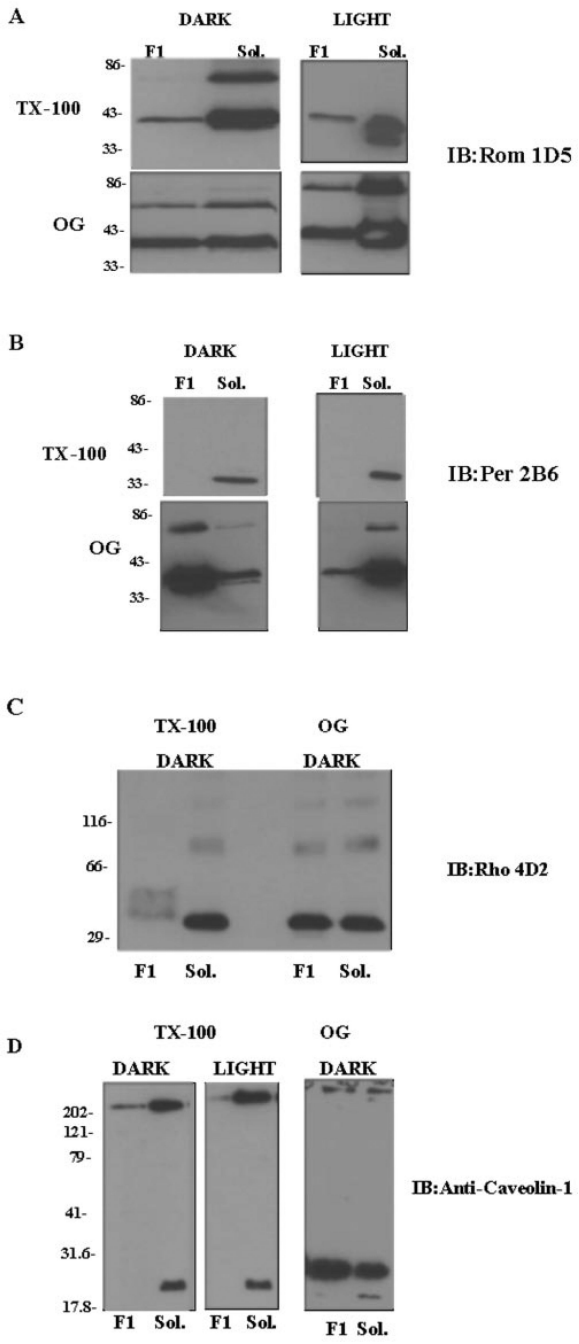

Fig. 1. Analysis of tetraspanin protein composition of membrane fractions isolated from Triton X-100- or OG-treated disk membranes by Western blot analysis

ROS disk membranes were treated with Triton X-100 (*TX-100*) or OG in the light or dark as indicated. Fractions corresponding to the low buoyant density band (*F1*) and to the soluble band (*Sol.*) were isolated and characterized as detailed in the legend to Table I. The proteins were separated by 10% SDS-PAGE in the presence of β-mercaptoethanol; electroblotted onto Immobilon-P membranes; and immunoblotted (*IB*) as indicated with anti-ROM-1 antibody 1D5 (*A*), anti-peripherin/rds (*Per*) antibody 2B6 (*B*), anti-rhodopsin (*Rho*) antibody 4D2 (*C*), and anti-caveolin-1 antibody (*D*).

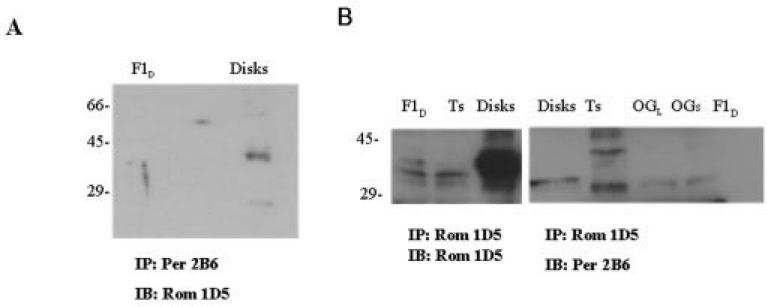

Fig. 2. Analysis of tetraspanin protein interactions within membrane fractions isolated from Triton X-100- or OG-treated disk membranes by immunoprecipitation

ROS disk membranes were treated with Triton X-100 or OG in the light or dark. Fractions corresponding to the low buoyant density band ($F1_D$) and to the soluble band (Triton X-100-soluble (*Ts*) and OG-soluble (*OGs*)) were isolated and characterized as detailed in the legend to Table I. Membrane fractions as indicated were with immunoprecipitated (*IP*) with anti-peripherin/rds (*Per*) antibody 2B6 and immunoblotted (*IB*) with anti-ROM-1 (*Rom*) mAb 1D5 (*A*) or immunoprecipitated with anti-ROM-1 mAb 1D5 and immunoblotted with anti-ROM-1 mAb 1D5 or anti-peripherin/rds antibody 2B6 (*B*).

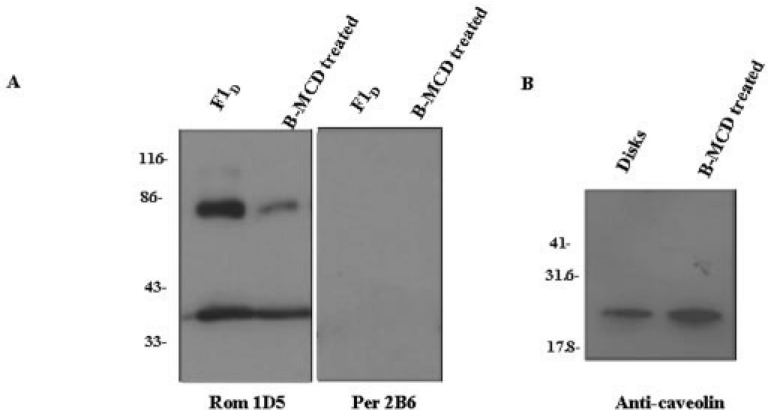

Fig. 3. Analysis of tetraspanin protein composition of cholesterol-depleted membrane fractions isolated from Triton X-100 by Western blot analysis

ROS disk membranes were treated with Triton X-100 in the dark. Fractions corresponding to the low buoyant density band ($F1_D$) were isolated and characterized as detailed in the legend to Table I. The fractions were treated with methyl-*β*-cyclodextran (*B-MCD*) to deplete membrane cholesterol. The cholesterol/phospholipid ratio in the treated samples was reduced by 50%. Samples were separated by 10% SDS-PAGE, transferred to nitrocellulose, and immunoblotted with anti-ROM-1 (*Rom*) mAb 1D5 or anti-peripherin/rds (*Per*) antibody 2B6 (*A*) or anti-caveolin-1 antibody (*B*).

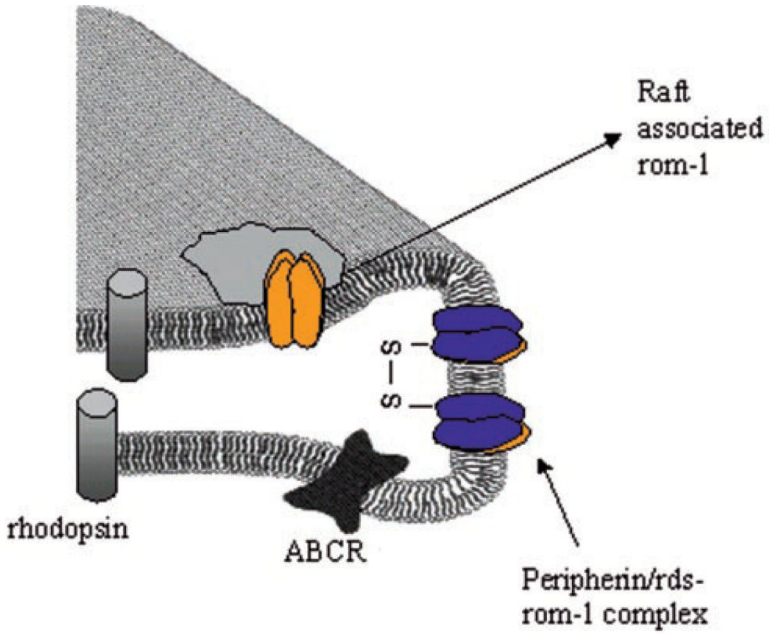

Fig. 4. Schematic representation of ROM-1 distribution in a membrane raft-like microdomain within the disk rim of ROS

Blue, peripherin/rds; *orange*, ROM-1.

Table I

Lipid profile of detergent-treated membranes

Samples	Sucrose (w/v)	Chol/PL (mol/mol)	SPH/PL (mol/mol)	Total phosphate
	%			%
Light				
Triton $F1_L$	18.6 ± 1.81	0.24 ± 0.09	0.11 ± 0.04	16.7 ± 2.4
Triton-soluble	26.0 ± 2.20	0.105 ± 0.02	0.03 ± 0.005	83 ± 6.8
OG $F1_L$	16.5 ± 3.80	0.13 ± 0.02	0.0079 ± 0.002	30 ± 4.6
OG-soluble	24.5 ± 3.80	0.101 ± 0.03	0.029 ± 0.001	70 ± 6.2
Dark				
Triton $F1_D$	20.3 ± 2.20	0.24 ± 0.07	0.10 ± 0.02	19 ± 3.4
Triton-soluble	26.5 ± 1.40	0.08 ± 0.02	0.03 ± 0.006	89 ± 2.6
OG $F1_D$	19.7 ± 0.76	0.12 ± 0.03	0.009 ± 0.003	26 ± 3.8
OG-soluble	27.0 ± 1.00	0.09 ± 0.01	0.031 ± 0.004	74 ± 5.9

Samples were treated with Triton X-100 or OG in the dark or light as indicated. The low buoyant density bands are designated F1, and the soluble fractions are indicated as Sol. The samples were assayed for cholesterol (Chol), phospholipid (PL), and sphingomyelin (SPH) as described under “Experimental Procedures.” The results are the means ± S.D. of nine independent preparations.